Tetrafluorophosphate Anion

Karl O. Christe,*[,1,2] David A. Dixon,[3] Gary J. Schrobilgen,*[,4] and William W. Wilson[1]

Contribution from Hughes STX, Propulsion Directorate, Phillips Laboratory, Edwards Air Force Base, California 93524, Loker Hydrocarbon Research Institute, University of Southern California, Los Angeles, California 90089, Pacific Northwest National Laboratory, Richland, Washington 99352, and Department of Chemistry, McMaster University, Hamilton, Ontario L8S 4MI, Canada

Received September 30, 1996[⊗]

Abstract: The elusive POF_4^- anion has been characterized for the first time. It is formed from $N(CH_3)_4F$ and POF_3 in CHF_3 solution at −140 °C and can be observed at this temperature by ^{19}F and ^{31}P NMR spectroscopy. Between −140 and −100 °C it reacts with POF_3 forming the $OF_2P-O-PF_5^-$ anion, which, at higher temperatures, reacts with F^- anions to give $PO_2F_2^-$ and PF_6^-. This reaction sequence provides a low activation energy barrier pathway for the highly exothermic dismutation of pseudo-trigonal-bipyramidal POF_4^- to tetrahedral $PO_2F_2^-$ and octahedral PF_6^- and explains the previous failures to isolate POF_4^- salts. In addition to POF_4^-, $OF_2POPF_5^-$, and $PO_2F_2^-$, the protonated form of $OF_2POPF_5^-$, i.e., HOF_2POPF_5, was also identified as a byproduct by NMR spectroscopy. The structure, vibrational spectra, force field, NMR parameters, and dismutation energy of POF_4^- were calculated by *ab initio* electronic structure methods using, where required, the closely related and well-known PF_4^- ion and POF_3, PF_3, SOF_4, and SF_4 molecules for the determination of scaling factors. Although the structures and dismutation energies of isoelectronic POF_4^- and SOF_4 are very similar, their dismutation behavior is strikingly different. While POF_4^- dismutates rapidly at low temperatures, SOF_4 is kinetically stable toward dismutation to SO_2F_2 and SF_6. This fact is attributed to the lack of a low activation energy barrier pathway for SOF_4. Furthermore, the dismutation energy calculations for POF_4^-, SOF_4, and $ClOF_3$ revealed very large errors in the previously published thermodynamic data for the heats of formations of SO_2F_2 and SOF_4 and the dismutation reaction energy of POF_4^-. Energy barriers and the C_{4v} transition states for the Berry-style pseudorotational exchange of equatorial and axial fluorines in POF_4^-, SOF_4, PF_4^-, and SF_4 were also calculated and can account for the observation that on the NMR time scale the exchange in PF_4^- and SF_4 can be frozen out at about −40 °C, while in POF_4^- and SOF_4 it is still rapid at −140 and −150 °C, respectively.

Introduction

On the basis of ion cyclotron resonance measurements[5,6] and ab initio calculations,[7] the F^- affinity of POF_3 exceeds that of PF_3 by about 8 and 16 kcal mol^{-1}, respectively. Our recent synthesis of $N(CH_3)_4PF_4$ from $N(CH_3)_4F$ and PF_3 in CH_3CN solution[8] and its surprisingly high thermal stability up to 150 °C strongly suggested that the closely related, but yet unknown, POF_4^- anion could also be isolated. This suggestion was also supported by the fact that the corresponding isoelectronic sulfur compounds, SF_4 and SOF_4, are both well-known and stable.[9] Consequently, one would predict that POF_3 should readily add a fluoride ion to form a pseudo-trigonal-bipyramidal POF_4^- anion with a C_{2v} structure similar to that of SOF_4.[10,11]

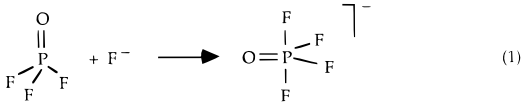

(1)

Previous attempts to prepare $CsPOF_4$ from CsF and POF_3 either without solvent at 130 °C or in CH_3CN at 50 °C resulted only in equimolar mixtures of $CsPO_2F_2$ and $CsPF_6$.[12]

$$2CsF + 2POF_3 \rightarrow CsPO_2F_2 + CsPF_6 \qquad (2)$$

In a recent ^{19}F and ^{31}P NMR study of the hydrolysis of $AgPF_6$ in CD_2Cl_2, signals (^{19}F: doublet at −85.8, $^1J_{P-F} = 1016$ Hz; ^{31}P: triplet at −2.4, −10.9, −19.2 with intensities characteristic of a quintet, rather than a triplet) were observed which, as will be obvious from our results, were erroneously attributed to POF_4^-.[13] The free gaseous POF_4^- ion has been observed as a stable intermediate in an ion cyclotron resonance (ICR) study[6] in which PF_5 was reacted with *tert*-butoxide to give POF_4^- (reaction 3),

$$t\text{-}C_4H_9O^- + PF_5 \rightarrow POF_4^- + t\text{-}C_4H_9F \qquad (3)$$

which then transferred F^- to PF_5 to give PF_6^- and POF_3 (reaction 4).

$$POF_4^- + PF_5 \rightarrow POF_3 + PF_6^- \qquad (4)$$

The POF_3 can also react with the *tert*-butoxide anion to give $PO_2F_2^-$ (reaction 5).

⊗ Abstract published in *Advance ACS Abstracts,* April 15, 1997.

(1) Hughes STX.
(2) University of Southern California.
(3) Pacific Northwest Laboratories.
(4) McMaster University.
(5) Larson, J. W.; McMahon, T. B. *J. Am. Chem. Soc.* **1983**, *105*, 2944.
(6) Larson, J. W.; McMahon, T. B. *Inorg. Chem.* **1987**, *26*, 4018.
(7) Dixon, D. A.; Christe, K. O. Unpublished results.
(8) Christe, K. O.; Dixon, D. A.; Mercier, H. P. A.; Sanders, J. C. P.; Schrobilgen, G. J.; Wilson, W. W. *J. Am. Chem. Soc.* **1994**, *116*, 2850.
(9) Greenwood, N. N.; Earnshaw, A. *Chemistry of the Elements*; Pergamon Press: Oxford, 1986.
(10) Oberhammer, H.; Boggs, J. E. *J. Mol. Struct.* **1979**, *56*, 107 and references cited therein.
(11) Hargittai, I. *J. Mol. Struct.* **1979**, *56*, 301.
(12) (a) Lustig, M.; Ruff, J. K. *Inorg. Chem.* **1967**, *6*, 2115. (b) **Note Added in Proof**: Prof. R. Schmutzler has brought a British Patent (1,104,244, Feb 21, 1968), which was issued to Barry Tittle, to our attention, in which $KPOF_4$ and $CsPOF_4$ were claimed as stable salts. This is an erroneous claim, as shown by our study.
(13) Fernandez-Galan, R.; Manzano, B. R.; Otero, A.; Lanfranchi, M.; Pellinghelli, M. A. *Inorg. Chem.* **1994**, *33*, 2309.

S0002-7863(96)03421-X CCC: $14.00

$$POF_3 + t\text{-}C_4H_9O^- \rightarrow PO_2F_2^- + t\text{-}C_4H_9F \quad (5)$$

Although the final products of these ion cyclotron resonance reactions, $PO_2F_2^-$ and PF_6^-, were the same as those in the dismutation reaction 2, their formation involved the *tert*-butoxide ion and not two POF_4^- anions, which would be unlikely to react with each other in the gas phase. Based on the relative F^- ion affinities, determined from the ICR reactions, the dismutation reaction 6

$$2POF_4^- \rightarrow PO_2F_2^- + PF_6^- \quad (6)$$

was estimated[6] to be exothermic by 76 kcal mol^{-1}, with $PO_2F_2^-$ and PF_6^- being the thermodynamically favored products. This seemed in sharp contrast to isoelectronic SOF_4 for which, based on the published thermodynamic values for SOF_4,[14,15] SO_2F_2,[16−18] and SF_6,[16] the analogous dismutation reaction 7

$$2SOF_4 \rightarrow SO_2F_2 + SF_6 \quad (7)$$

would be about thermally neutral. This huge energy difference for two isoelectronic systems was puzzling and needed either verification or rationalization.

In view of these challenges, it was interesting to attempt the synthesis and characterization of a POF_4^- salt, to elucidate the mechanism and energy of its dismutation reaction 6, and to study its fluxionality and axial and equatorial fluorine ligand exchange.[8]

Experimental Section

Apparatus and Materials. Volatile materials were handled on either a flamed-out Pyrex glass vacuum line equipped with Kontes glass-Teflon valves and a Heise pressure gauge or a nickel/stainless steel vacuum line equipped with MKS type 122A pressure transducers (0−1000 Torr, ±0.5% of reading) having fluorine passivated Inconel as the wetted surface and a model PDR-5B five-channel digital readout and power supply. Nonvolatile materials were handled in the dry nitrogen atmosphere of a glovebox. The infrared and Raman spectrometers have previously been described.[19] Literature methods were used for the syntheses of $N(CH_3)_4F$[20] and POF_3[21,22] and the drying of CH_3CN.[23,24] CHF_3 (The Matheson Co. or Canadian Liquid Air) and SO_2 (The Matheson Co.) were purified by fractional condensation prior to their use.

Nuclear Magnetic Resonance Spectroscopy. The ^{19}F (282.409 MHz) and ^{31}P (121.497 MHz) NMR spectra were recorded unlocked (field drift <0.1 Hz h^{-1}) without spinning on a Bruker AM 300 spectrometer equipped with a 7.0463 T cryomagnet and a 5-mm $^1H/^{13}C/^{19}F/^{31}P$ combination probe. Free induction decays were typically accumulated in 64K (^{19}F) and 32K (^{31}P) memories. In the case of ^{31}P spectra, a Gaussian line shape function was applied for resolution enhancement prior to zero filling the free induction decay into a 128K memory. Spectral width settings of 50 (^{19}F) and 30 kHz (^{31}P) were employed, yielding data point resolutions of 1.53 (^{19}F) and 1.80 Hz or 0.45 Hz for resolution enhanced spectra (^{31}P) and acquisition times of 0.328 (^{19}F) and 0.557 s (^{31}P), respectively. Relaxation delays were not applied. Typically, 10 000 transients were accumulated. Pulse widths were 1.0 (^{19}F) and 3.0 μs (^{31}P). Line broadening parameters used in the exponential multiplication of the free induction decays were 0.5 (^{19}F) and −4.0 Hz with a Gaussian block parameter of 0.5 for Gaussian multiplication (^{31}P). Temperatures were measured with a copper−constantan thermocouple inserted directly into the probe, are considered accurate to ±1 °C, and were constant to less than ±0.1 °C. The spectra were referenced to neat external samples of $CFCl_3$ (^{19}F) and 85% H_3PO_4 (^{31}P) at ambient temperature, and the IUPAC sign convention for chemical shifts was used.

Samples for NMR spectroscopy were prepared in medium-wall Pyrex glass NMR tubes (Wilmad). The tubes were fused to 3-cm lengths of 0.25-in. o.d. glass tubing and joined to J. Young glass/Teflon valves through 0.25-in. 316 stainless steel Cajon Ultra Torr unions and dried overnight by pumping on a glass vacuum line. Weighed amounts of $N(CH_3)_4F$ were loaded into the NMR tubes in the drybox and then transferred to a calibrated metal vacuum manifold where CHF_3 solvent (ca. 0.25 mL) followed by a known pressure of POF_3 were condensed at −196 °C onto $N(CH_3)_4F$, before flame sealing the tubes. The following sample compositions, $N(CH_3)_4F:POF_3 = 0.495$, 0.899, 0.957, and 3.56, were studied.

Attempted Bulk Synthesis of $N(CH_3)_4POF_4$. A weighed amount of anhydrous $N(CH_3)_4F$ was placed inside the drybox into a prepassivated (with ClF_3) Teflon-FEP container which was closed by a stainless steel valve. On the vacuum line, POF_3 and CHF_3 (large excess) were added to the Teflon container at −196 °C. The mixture was warmed to −140 °C with agitation and kept at this temperature for 2 h. Attempts to isolate solid $N(CH_3)_4POF_4$ by removal of the CHF_3 solvent under vacuum at −126 °C produced a white solid of the correct weight expected for $N(CH_3)_4POF_4$, but its vibrational spectra recorded at room temperature showed an equimolar mixture of $N(CH_3)_4PO_2F_2$ and $N(CH_3)_4PF_6$. When this reaction was repeated either in other solvents, such as SO_2 at −78 °C, POF_3 at −64 °C, or CH_3CN at −31 °C, or without a solvent at 25 °C with use of 2 Torr of gaseous POF_3 in a flamed out glass bulb, again only the dismutation products $N(CH_3)_4PO_2F_2$ and $N(CH_3)_4PF_6$ were observed as final room-temperature stable products.

Computational Methods. A variety of electronic structure calculations were performed in order to calculate the geometries, relative energies, and vibrational frequencies of the phosphorus and sulfur species. The electronic structure calculations were done at a number of different levels. The first set of calculations were done at the Hartree−Fock (HF) level with the program GRADSCF on Cray YMP and C90 computer systems.[25] A polarized double-ζ valence basis set (DZP) from Dunning and Hay[26] was used for F and O, and the McLean and Chandler sets[27] (6s/4p) were used for S and P augmented by d(P) = 0.5 and d(S) = 0.6. Subsequently, the DZP basis set was augmented by a set of diffuse p functions on all atoms (DZP+) with the following exponents: p(O) = 0.059, p(F) = 0.074, p(P) = 0.035, and p(S) = 0.041. The geometries and frequencies of the lowest energy species were calculated at this level by using analytic derivative methods.[28,29] The HF/DZP+ second derivative results were used to calculate the molecular force fields with the program BMATRIX.[25]

(14) Dittmer, G.; Niemann, U. *Philips J. Res.* **1982**, *37*, 1.
(15) Herron, J. T. *J. Phys. Chem. Ref. Data* **1987**, *16*, 1.
(16) Stull, D. R.; Prophet, H. *JANAF Thermochemical Tables*, 2nd ed.; U.S. GPO, Washington, DC, 1971; 1978 Supplement. *J. Phys. Chem. Ref. Data* **1978**, *7*, 793.
(17) Chase, M. W., Jr.; Curnett, J. L.; Downey, J. R., Jr.; McDonald, R. A.; Syverud, A. N.; Valenzuela, E. A. *J. Phys. Chem. Ref. Data* **1982**, *11*, 695.
(18) Reese, R. M.; Dibeler, V. H.; Franklin, J. L. *J. Chem. Phys.* **1958**, *29*, 880.
(19) Christe, K. O.; Wilson, W. W.; Bau, R.; Bunte, S. W. *J. Am. Chem. Soc.* **1992**, *114*, 3411.
(20) Christe, K. O.; Wilson, W. W.; Wilson, R. D.; Bau, R.; Feng, J. *J. Am. Chem. Soc.* **1990**, *112*, 7619.
(21) Christe, K. O.; Gnann, R.; Wagner, R. I.; Wilson, W. W. *Eur. J. Solid State Inorg. Chem.* **1996**, *33*, 865.
(22) Kwasnik, W. In *Handbook of Preparative Inorganic Chemistry*, 2nd ed.; Brauer, G., Ed.; Academic Press: New York, 1963; Vol. 1, Section 4, pp 193−194.
(23) Christe, K. O.; Dixon, D. A.; Mahjoub, A. R.; Mercier, H. P. A.; Sanders, J. C. P.; Seppelt, K.; Schrobilgen, G. J.; Wilson, W. W. *J. Am. Chem. Soc.* **1993**, *115*, 2696.
(24) Winfield, J. M. *J. Fluorine Chem.* **1984**, *25*, 91.
(25) GRADSCF is an ab initio program system designed and written by A. Komornicki at Polyatomics Research, Mountain View, CA. BMATRIX is an auxiliary program used for force constant analysis.
(26) Dunning, T. H., Jr.; Hay, P. J. In *Methods of Electronic Structure Theory*; Schaefer, H. F., III, Ed.; Plenum Press: New York, 1977; Chapter 1.
(27) McLean, A. D.; Chandler, G. S. *J. Chem. Phys.* **1980**, *72*, 5369.
(28) (a) Komornicki, A.; Ishida, K.; Morokuma, K.; Ditchfield, R.; Conrad, M. *Chem. Phys. Lett.* **1977** *45*, 595. (b) McIver, J. W., Jr.; Komornicki, A. *Chem. Phys. Lett.* **1971**, *10*, 202. (c) Pulay, P. In *Applications of Electronic Structure Theory*; Schaefer, H. F., III, Ed.; Plenum Press: New York, 1977; p 153. (d) Breidung, J.; Thiel, W.; Komornicki, A. *Chem. Phys. Lett.* **1988**, *153*, 76.
(29) (a) King, H. F.; Komornicki, A. *J. Chem. Phys.* **1986**, *84*, 5465. (b) King, H. F.; Komornicki, A. In *Geometrical Derivatives of Energy Surfaces and Molecular Properties*; Jorgenson, P., Simons, J., Eds.; NATO ASI Series C. Vol. 166; D. Reidel: Dordrecht, 1986; p 207.

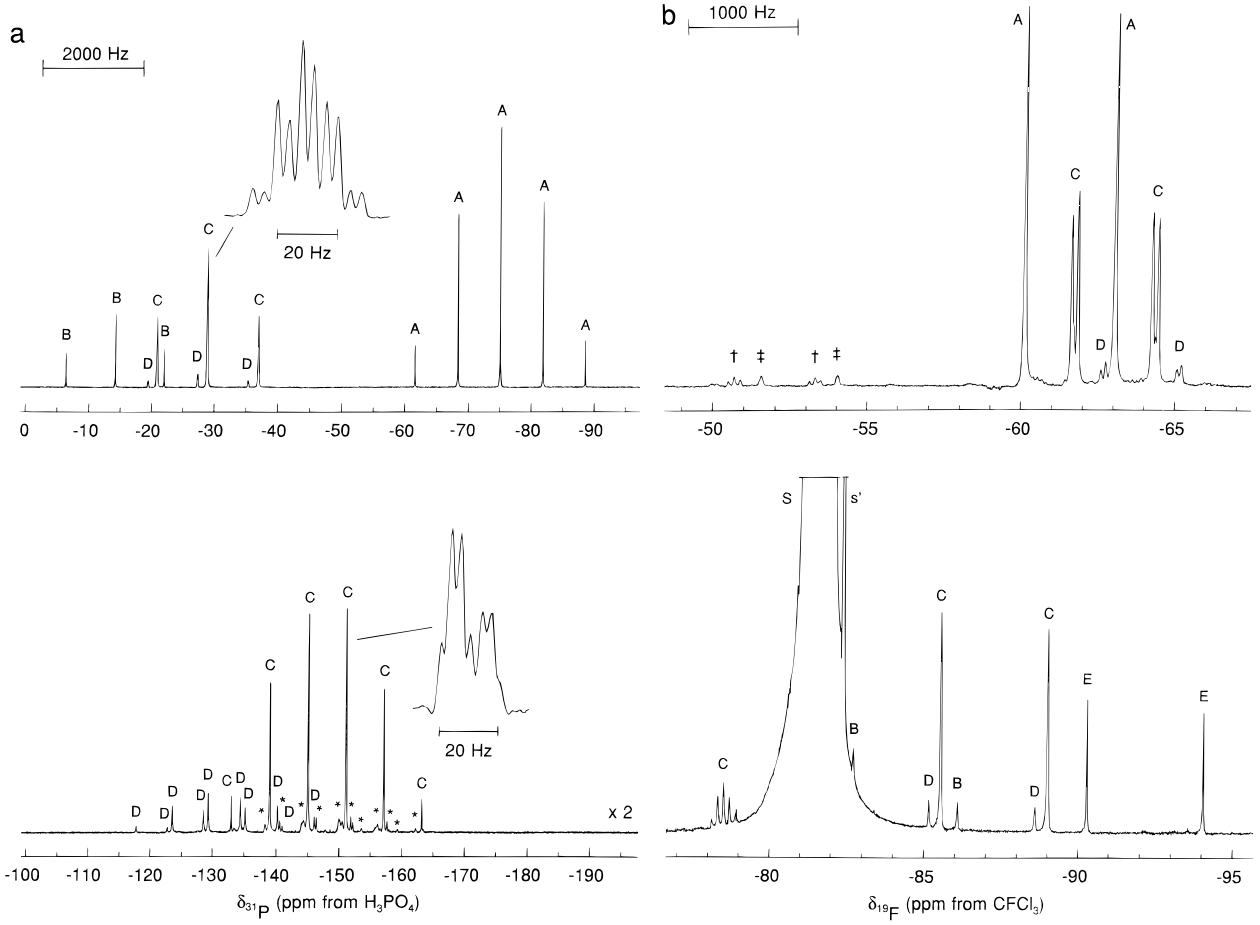

Figure 1. NMR spectra (7.0463 T) of a 0.90:1.00 molar ratio of POF_3:$N(CH_3)_4F$ recorded in CHF_3 solvent at −140 °C: (a) ^{31}P spectrum (121.497 MHz) and (b) ^{19}F spectrum (282.409 MHz). The labeling scheme is as follows: (A) POF_4^-, (B) $PO_2F_2^-$, (C) $OF_2P-O-PF_5^-$, (D) $HOF_2P-O-PF_5$, (E) POF_3, (S) CHF_3 solvent. Peaks denoted by (*), (†), and (‡) are unassigned. Expansions in the ^{31}P spectrum of $OF_2P-O-PF_5^-$ (C) represent multiplet fine structures visible under high resolution on each branch of the triplet and pseudosextet (doublet of quintets) arising from the P_A and P_B environments, respectively, in structure **A**.

Subsequent calculations on various conformers of the four molecular species were done with the program Gaussian94 on an SGI Indigo2.[30] The basis set was of polarized double-ζ valence quality with the same basis set for F and O given above and the (5s/3p) set of McLean and Chandler augmented by the same d functions given above. The optimized HF geometries were used to calculate the MP2 energies[31] at the frozen core level. The HF/DZVP geometries were used to calculate NMR chemical shifts at the nonlocal BLYP level with the nonlocal exchange potential of Becke[32] and the nonlocal correlation potential of Lee, Yang, and Parr.[33] The basis set for the NMR calculations was of triple-ζ form[27,34] augmented by two sets of d polarization functions each formed from two Gaussian functions and an f polarization function. The origin problem for the NMR chemical shift calculations was handled by using the GIAO method.[35] In order to compare to experiment, the following standards were used: CCl_3F for F, $[PO_4]^{3-}$ for P, and H_2O for O. The difference in the shift from the standard is reported.

Density functional calculations were done with the program DGauss[36] at the local (LDFT) level with a polarized double-ζ basis set (DZVP2).[37] The local potential fit of Vosko, Wilk, and Nusair[38] was used. Geometries were optimized at this level and frequencies were calculated by analytic derivative methods.[39] These geometries were used to calculate the NMR chemical shifts[40] at the IGLO[41] and LORG levels.[42]

In order to calculate the dismutation reaction energies, additional calculations were done. All calculations were done with the HF geometries. The additional calculations were done with the correlation-consistent basis sets[43,44] at the cc-VDZ and aug-cc-VTZ levels at the

(30) *Gaussian 94*: Frisch, M. J.; Trucks, G. W.; Schlegel, H. B.; Gill, P. M. W.; Johnson, B. G.; Robb, M. A.; Cheeseman, J. R.; Keith, T. A.; Petersson, G. A.; Montgomery, J. A.; Raghavachari, K.; Al-Laham, M. A.; Zakrzewski, V. G.; Ortiz, J. V.; Foresman, J. B.; Cioslowski, J.; Stefanov, B. B.; Nanayakkara, A.; Challacombe, M.; Peng, C. Y.; Ayala, P. Y.; Chen, W.; Wong, M. W.; Andres, J. L.; Replogle, E. S.; Gomperts, R.; Martin, R. L.; Fox, D. J.; Binkley, J. S.; Defrees, D. J.; Baker, J.; Stewart, J. J. P.; Head-Gordon, M.; Gonzalez, C.; Pople, J. A., Gaussian, Inc.; Pittsburgh, PA, 1995.

(31) (a) Møller, C.; Plesset, M. S. *Phys. Rev.* **1934**, *46*, 618. (b) Pople, J. A.; Binkley, J. S.; Seeger, R. *Int. J. Quantum Chem. Symp.* **1976**, *10*, 1. Pople, J. A.; Krishnan, R.; Schlegel, H. B.; Binkley, J. S. *Int. J. Quantum Chem. Symp.* **1979**, *13*, 325. Handy, N. C.; Schaefer, H. F., III *J. Chem. Phys.* **1984**, *81*, 5031.

(32) (a) Becke, A. D. *Phys. Rev. A* **1988**, *38*, 3098. (b) Becke, A. D. In *The Challenge of d and f Electrons: Theory and Computation*; Salahub, D. R., Zerner, M. C., Eds.; ACS Symposium Series, No. 394; American Chemical Society: Washington, DC, 1989; p 166. (c) Becke, A. D. *Int. J. Quantum Chem. Symp.* **1989**, *23*, 599.

(33) Lee, C.; Yang, W.; Parr, R. G. *Phys, Rev. B* **1988**, *37*, 785.

(34) Dunning, T., Jr. *J. Chem. Phys.* **1971**, *55*, 716.

(35) Cheeseman, J. R.; Trucks, G. W.; Keith, T. A.; Frisch, M. J. *J. Chem. Phys.* **1996**, *104*, 5497. London, F. *J. Phys, Radium (Paris)* **1937**, *8*, 397. Ditchfield, R. *Mol. Phys.* **1974**, *27*, 789. Wolinski, K.; Hinton, J. F.; Pulay, P. *J. Am. Chem. Soc.* **1990**, *112*, 8251.

(36) (a) Andzelm, J.; Wimmer, E.; Salahub, D. R. In *The Challenge of d and f Electrons: Theory and Computation*; Salahub, D. R., Zerner, M. C., Eds.; ACS Symposium Series, No. 394; American Chemical Society: Washington, DC, 1989; p 228. (b) Andzelm, J. In *Density Functional Theory in Chemistry*; Labanowski, J., Andzelm, J., Eds.; Springer-Verlag: New York, 1991; p 155. (c) Andzelm, J. W.; Wimmer, E. *J. Chem. Phys.* **1992**, *96*, 1280. DGauss is a density functional program available from Oxford Molecular.

(37) Godbout, N.; Salahub, D. R.; Andzelm, J.; Wimmer, E. *Can. J. Chem.* **1992**, *70*, 560.

(38) Vosko, S. J.; Wilk, L.; Nusair, W. *Can J. Phys.* **1980**, *58*, 1200.

(39) Komornicki, A.; Fitzgerald, G. *J. Phys. Chem.* **1993**, *98*, 1398 and references therein.

(40) Arduengo, A. J., III; Dixon, D. A.; Kumashiro, K. K.; Lee, C.; Power, W. P.; Zilm, K. W. *J. Am. Chem. Soc.* **1994**, *116*, 6361.

(41) (a) Kutzelnigg, W. *Isr. J. Chem.* **1980**, *19*, 193. (b) Schindler, M.; Kutzelnigg, W. *J. Chem. Phys.* **1982**, *76*, 1919.

(42) Hansen, A. E.; Bouman, T. D. *J. Chem. Phys.* **1985**, *82*, 5035.

Table 1. NMR Parameters for the POF_4^-, $PO_2F_2^-$, and $OF_2POPF_5^-$ Anions and POF_3 and HOF_2POPF_5 in CHF_3 solution at −140 °C

	$\delta(^{31}P)$, ppm		$\delta(^{19}F)$, ppm			coupling constants, Hz								
species[a]	P_A	P_B	F_a	F_b	F_c	^1J ($^{31}P_A-^{19}F_a$)	^1J ($^{31}P_B-^{19}Fb$)	^1J ($^{31}P_B-^{19}F_c$)	^2J ($^{31}P_A-^{31}P_B$)	^2J ($^{31}P_A-^{1}H$)	^2J ($^{19}F_b-^{19}F_c$)	^3J ($^{31}P_A-^{19}F_b$)	^3J ($^{31}P_A-^{19}F_c$)	^4J ($^{19}F_a-^{19}F_b$)
POF_4^-		−75.1 (quin)[b]		−61.6 (d)		819								
POF_3		−33.9 (quar)		−92.1 (d)		1061								
$PO_2F_2^-$		−14.2 (tr)		−84.4 (d)		948								
$OF_2POPF_5^-$	−28.9 (tr, quin, d)	−148.1 (d, quin, d, tr)[c]	−87.3 (d)	−63.0 (d, d)	−79.8 (d, quin)[d]	979	736	729	3		55.3	7.4	3.9	3
HOF_2POPF_5	−27.4 (tr, d, m)	−131.9 (d, quin, d, tr)	−86.9 (d)	−63.9 (d, d)	not obsd[e]	968	706	614		12	41.0			

[a] For a definition of the individual atoms see structures **A** and **B**. [b] d = doublet, tr = triplet, quar = quartet, quin = quintet, m = unresolved. [c] The similarity of $^1J(^{31}P_B-^{19}F_b)$ and $^1J(^{31}P_B-^{19}F_c)$ causes the expected doublet of quintets to have the appearance of a sextet. [d] Only one of the two quintets was observed; the second one was obscured by the solvent peak; the listed δ value was obtained from the position of the observed quintet and the known $^1J(^{31}P_B-^{19}F_c)$ value. [e] Probably obscured by the CHF_3 solvent peak.

MP2 level. In addition, higher levels of correlation were examined at the coupled cluster single and double excitation with a correction for triples (CCSD(T)) level[45] with the cc-VDZ basis set. The CCSD(T) calculations were done with the program MOLPRO.[46]

Results and Discussion

Synthesis and Properties of $N(CH_3)_4POF_4$. The synthesis of POF_4^- salts is very difficult and was achieved only from a soluble F^- ion source[20] and POF_3 in an inert solvent, such as CHF_3, at temperatures of about −140 °C.

$$N(CH_3)_4F + POF_3 \xrightarrow[-140\ °C]{CHF_3} N(CH_3)_4POF_4 \qquad (8)$$

Even at this low temperature, the POF_4^- anion already starts to dismutate according to (6), and at elevated temperatures equimolar mixtures of $PO_2F_2^-$ and PF_6^- salts are observed as the only products. Thus, our attempts to isolate solid $N(CH_3)_4POF_4$ from solutions of $N(CH_3)_4F$ and POF_3 in CHF_3 at −126 °C, SO_2 at −78 °C, POF_3 at −64 °C, or CH_3CN at −31 °C produced only the dismutation products. Similarly, a solvent-free reaction of $N(CH_3)_4F$ with 2 Torr of gaseous POF_3 at 35 °C did not result in POF_4^- formation. In view of these difficulties, $N(CH_3)_4POF_4$ could not be isolated as a stable solid and was characterized by its multinuclear NMR spectra in CHF_3 solution at −140 °C (see below). These results are in accord with the earlier report[12] that CsF and POF_3 in CH_3CN at 50 °C produced only $CsPO_2F_2$ and $CsPF_6$.

^{19}F and ^{31}P NMR Spectroscopy. The ^{19}F and ^{31}P NMR spectra of about equimolar mixtures of $N(CH_3)_4F$ and POF_3 recorded at −140 °C in CHF_3 (Figure 1 and Table 1) consist of several first-order multiplet patterns. An intense quintet centered at −75.1 ppm in the ^{31}P NMR spectrum is assigned to the POF_4^- anion and has its doublet counterpart in the ^{19}F NMR spectrum at −61.6 ppm with $^1J(^{31}P-^{19}F) = 819$ Hz (peaks A in Figure 1). Although POF_4^- is expected to have a trigonal-bipyramidal geometry like the isoelectronic SOF_4 molecule, with the oxygen and two fluorines occupying the equatorial plane and two fluorines occupying the axial positions,[10,11] the limiting spectrum in which the axial and equatorial fluorines are inequivalent was not observed at −140 °C. Rather, the spectra show that the POF_4^- anion, like SOF_4,[47] is fluxional on the NMR time scale (see below).

A second major species (peaks B in Figure 1) exhibits a triplet at −14.2 ppm in the ^{31}P NMR spectrum and a doublet at −84.4 ppm in the ^{19}F NMR spectrum [$^1J(^{31}P-^{19}F) = 948$ Hz] and is assigned to the previously characterized $PO_2F_2^-$ anion.[13,48,49] Resonances assigned to unreacted POF_3 (^{19}F, −92.1 ppm, doublet (peaks E in Figure 1); ^{31}P, −33.9 ppm, quartet (not shown in Figure 1); $^1J(^{31}P-^{19}F)$ 1061 Hz)[50,51] were also observed.

A fourth set of intense resonances (peaks C in Figure 1) is assigned to the oxygen-bridged $OF_2P-O-PF_5^-$ anion (structure **A**). The ^{19}F resonance of the POF_2 group occurs at −87.3 ppm

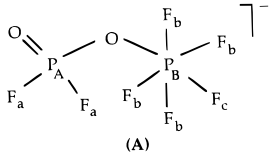

(A)

and is comprised of a doublet arising from coupling to the directly bonded phosphorus atom [$^1J(^{31}P_A-^{19}F_a) = 979$ Hz]. The PF_5 group displays an AX_4 pattern in the ^{19}F NMR spectrum with the doublet at −63.0 ppm and the quintet at −79.8 ppm [$^2J(^{19}F_b-^{19}F_c) = 55.3$ Hz]. Both multiplets are split into doublets by their respective one-bond couplings to phosphorus [$^1J(^{31}P_B-^{19}F_b) = 736$ Hz and $^1J(^{31}P_B-^{19}F_c) = 729$ Hz] (one set of the quintets is masked by the intense CHF_3 solvent doublet at −81.62 ppm). The ^{31}P NMR spectrum consists of two sets of intense complex multiplets. A triplet of quintets of doublets centered at −29.0 ppm is assigned to P_A and arises from $^1J(^{31}P_A-^{19}F_a)$, $^3J(^{31}P_A-^{19}F_b)$, and $^3J(^{31}P_A-^{19}F_c) = 3.9$ Hz. The multiplet at −148.1 ppm is assigned to P_B, which appears to be a sextet under low resolution conditions but is shown actually to be a severely overlapping doublet of quintets at higher resolution that arises from two nearly equal one-bond $^{31}P-^{19}F$ couplings, namely $^1J(^{31}P_B-^{19}F_b)$ and $^1J(^{31}P_B-^{19}F_c)$. Resolution enhancement using a Gaussian line fit reveals that each line of the doublet of quintets pattern is further split into an overlapping doublet of triplets arising from $^2J(^{31}P_A-^{31}P_B) = 3$ Hz and $^4J(^{19}F_a-^{19}F_b) = 3$ Hz to give a pseudoquartet. The $OF_2P-O-PF_5^-$ anion has been previously characterized by ^{19}F and ^{31}P NMR spectroscopy in CH_3CN solution,[48] and in view of the different solvent and large temperature difference, the NMR

(43) Dunning, T. H., Jr. *J. Chem. Phys.* **1989**, *90*, 1007.
(44) Kendall, R. A.; Dunning, T. H., Jr.; Harrison, R. J. *J. Chem. Phys.* **1992**, *96*, 6796.
(45) (a) Bartlett, R. J. *J. Phys. Chem.* **1989**, *93*, 1697. (b) Kucharski, S. A.; Bartlett, R. J. *Adv. Quantum Chem.* **1986**, *18*, 281. (c) Bartlett, R. J.; Stanton, J. F. In *Reviews of Computational Chemistry*; Lipkowitz, K. B., Boyd, D. B., Eds.; VCH Publishers: New York, 1995; Vol. V, Chapter 2, p 65.
(46) MOLPRO is a package of *ab initio* programs written by Werner, H.-J. and Knowles, P. J. with contributions from Almlof, J., Amos, R. D., Deegan, M. J. O., Elbert, S. T., Hampel, C., Meyer, W., Peterson, K. A., Pitzer, R. M., Stone, A. J., Taylor, P. R., and Lindh, R.
(47) Christe, K. O.; Schack, C. J.; Curtis, E. C. *Spectrochim. Acta, Part A* **1977**, *33A*, 323.
(48) Il'in, E. G.; Meisel, M.; Shcherbakova, M. N.; Wolf, G. U.; Buslaev, Yu. A. *Dokl. Akad. Nauk SSSR* **1982**, *266*, 878.
(49) Reddy, G. S.; Schmutzler, R. *Z. Naturforsch. Teil B* **1970**, *25b*, 1199.
(50) Moedritzer, K.; Maier, L.; Groenweghe, L. C. D. *J. Chem. Eng. Data* **1962**, *7*, 307.
(51) Gutowsky, H. S.; McCall, D. W.; Slichter, C. P. *J. Chem. Phys.* **1953**, *21*, 279.

parameters obtained in the present study are in good agreement with the published values (two spin−spin couplings not reported for the $OF_2P-O-PF_5^-$ anion in the previous study are reported in this study, i.e., $^2J(^{31}P_A-^{31}P_B)$ and $^3J(^{31}P_A-^{19}F_c)$).

Several weak multiplets also appear in the ^{19}F and ^{31}P NMR spectra at −140 °C. One set of multiplets (peaks D in Figure 1) is assigned to the protonated $OF_2P-O-PF_5^-$ anion, namely, $HOF_2P-O-PF_5$ (structure **B**). In the ^{31}P spectrum, a triplet

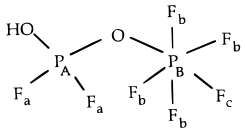

(B)

[$^1J(^{31}P_A-^{19}F_a) = 968$ Hz] of doublets [$^2J(^{31}P_A-^1H) = 12$ Hz] of unresolved multiplets due to P_A occurs at −27.4 ppm, and a doublet [$^2J(^{31}P_B-^{19}F_c) = 614$ Hz] of quintets [$^2J(^{31}P_B-^{19}F_b) = 706$ Hz] is observed for P_B. In the ^{19}F NMR spectrum, a doublet [$^1J(^{31}P_A-^{19}F_a)$] at −86.9 ppm due to the two F_a atoms and a doublet [$^1J(^{31}P_B-^{19}F_b)$] of doublets [$^2J(^{19}F_b-^{19}F_c) = 41$ Hz] at −63.9 ppm due to the four F_b atoms are observed. The doublet of quintets, expected for F_c, has not been observed because of its relative broadness, low intensity, and/or probable overlap with the strong CHF_3 solvent peak. Although the $^2J(^{31}P_A-^{31}P_B)$, $^3J(^{31}P_A-^{19}F_b)$, and $^3J(^{31}P_A-^{19}F_c)$ couplings were not observed under our resolution conditions because of their expected small magnitudes (cf. corresponding coupling constants for structure **A** in Table 1), the given assignments are tied together through either common coupling constants or constant relative intensities and growth patterns in different samples. The NMR parameters of the HOF_2PO group are in good agreement with those reported for $HOPOF_2$ in CH_3CN solvent at room temperature,[48] although $^2J(^{31}P-^1H)$ was not observed for $HOPOF_2$ in the previous study. In that study, the ^{31}P resonance of HPO_2F_2 occurred to slightly higher frequency of $PO_2F_2^-$ with ^{19}F shifts being almost the same, and similar trends are noted for $HOF_2P-O-PF_5$ and $OF_2P-O-PF_5^-$. The remaining very weak spectral features appearing in the ^{19}F and ^{31}P NMR spectra have not been assigned.

Warming a CHF_3 solution containing POF_4^- from −140 to −90 °C resulted in loss of the ^{19}F and ^{31}P resonances of POF_4^- with only the $PO_2F_2^-$ and $OF_2P-O-PF_5^-$ resonances remaining. The decomposition is in accord with global reaction 6 with POF_4^- dismutating to $PO_2F_2^-$ and PF_6^- by means of the intermediate dimeric $OF_2P-O-PF_5^-$ anion. Although no resonances attributed to the other dismutation product, PF_6^-, were observed in the ^{19}F and the ^{31}P spectra, the solution at −90 °C contained a white precipitate of what is presumably $N(CH_3)_4PF_6$. The formation of $N(CH_3)_4PF_6$ as a main product under these conditions was established by vibrational spectroscopy of the solid products.

A recent paper reports the preparation of POF_4^- by the hydrolysis of $AgPF_6$ in CD_2Cl_2 at room temperature.[13] The reported NMR parameters consist of a doublet in the ^{19}F NMR spectrum at −85.8 ppm, $^1J(^{31}P-^{19}F) = 1016$ Hz, and a triplet in the ^{31}P NMR spectrum, unconventionally reported in ppm at −2.4, −10.9, and −19.2, with relative intensities characteristic of a quintet rather than a triplet. The ^{31}P chemical shift and scalar coupling differ significantly from those determined for POF_4^- in the present work, and in fact, the $^{31}P-^{19}F$ coupling is more in line with that for tetracoordinate phosphorus.[49] Moreover, the reported stability of the species at ambient temperature is not in agreement with the observed thermal instability of POF_4^-.

The NMR parameters for POF_4^- follow several previously established trends[49−51] and are in accord with our expectations for this ion. The ^{19}F shielding decreases upon going from POF_3 [$\delta(^{19}F)$, −92.1 ppm] to POF_4^- [$\delta(^{19}F)$, −61.6 ppm] and from PF_3 [$\delta(^{19}F)$, −34.3 ppm[52]] to PF_4^- [average $\delta(^{19}F)$, −18.7 ppm[8]], and is a well-established trend for neutral fluorides and their fluoroanions.[53] This shielding trend is also found for neutral fluorides and their cations, as in the structurally related pairs SOF_3^+ [$\delta(^{19}F)$, 32 ppm[54]] > SOF_4 [$\delta(^{19}F)$, 75 ppm[54]], SF_3^+ [$\delta(^{19}F)$, 25.5 to 30.5 ppm[55]] > SF_4 [average $\delta(^{19}F)$, 95 ppm[56]], and SeF_3^+ [$\delta(^{19}F)$, 6.0 ppm[57]] > SeF_4 [average $\delta(^{19}F)$, 24.8 ppm[57]]. On the basis of the simple "atom-in-a-molecule" approach to the paramagnetic contribution to nuclear shielding,[58] the lowest molecular excitation energy is expected to increase with increasing positive charge so that the paramagnetic contribution to the shielding increases. Apparently, the effect of increased E−F bond order in the more positively charged species, which causes greater deviations from the spherical symmetry of F^- and a larger paramagnetic contribution, is offset by the larger molecular excitation term. The opposite trend is noted in the ^{31}P shieldings, which increase in the order POF_3 [$\delta(^{31}P)$, −33.9 ppm] < POF_4^- [$\delta(^{31}P)$, −75.1 ppm] and PF_3 [$\delta(^{31}P)$, 103.5 ppm[59]] < PF_4^- [$\delta(^{31}P)$, 42.3 ppm[8]], and is also observed for the ^{77}Se shieldings SeF_3^+ [$\delta(^{77}Se)$, 1122 ppm[60]] < SeF_4 [$\delta(^{77}Se)$, 1082 ppm[60]]. Decreases in central element shielding with decreasing coordination number are general and correlate with increasing p-orbital populations associated with a more highly positive (electronegative) central atom.[58]

The $^1J(^{31}P-^{19}F)$ coupling decreases in the order POF_3 (1061 Hz) > POF_4^- (819 Hz). Analogous trends are observed for PF_3 (1401 Hz[59]) > PF_4^- (average, 1032 Hz[8]) and for the $^1J(^{77}Se-^{19}F)$ couplings of SeF_3^+ (1213 Hz[57]) > SeF_4 (average, 745 Hz[61]), which are consistent with a decrease in the bond order for the more polar P−F and Se−F bonds of POF_4^-, PF_4^-, and SeF_4 relative to those of POF_3, PF_3, and SeF_3^+, respectively. The magnitudes of the scalar couplings can be correlated to the s-electron densities at the spin-coupled nuclei for a Fermi contact dominated spin−spin coupling mechanism.[62] The decrease in scalar coupling is consistent with the anticipated decrease in s-character with increasing bond polarity and coordination number.

Fluxionality in POF_4^- and SOF_4. The POF_4^- anion, like its isoelectronic analog, SOF_4,[47,63] undergoes rapid intramolecular exchange of its axial and equatorial fluorines. The mechanism by which the intramolecular ligand exchange process occurs in POF_4^- and SOF_4 is most likely the classical Berry pseudorotation mechanism[64] involving a pyramidal C_{4v} transition

(52) Muetterties, E. L.; Phillips, W. D. *J. Am. Chem. Soc.* **1957**, *79*, 322.
(53) Jameson, C. J. In *Multinuclear NMR*; Mason, J., Ed.; Plenum Press: New York, 1987; Chapter 16, p 441.
(54) Brownstein, M.; Dean, P. A. W.; Gillespie, R. J. *Chem. Commun.* **1970**, 9.
(55) Azeem, M.; Brownstein, M.; Gillespie, R. J. *Can. J. Chem.* **1969**, *47*, 4159.
(56) Muetterties, E. L.; Phillips, W. D. *J. Am. Chem. Soc.* **1959**, *81*, 1084.
(57) Brownstein, M.; Gillespie, R. J. *J. Chem. Soc., Dalton Trans.* **1973**, 67.
(58) Jameson, C. J.; Mason, J. In *Multinuclear NMR*; Mason, J., Ed.; Plenum Press: New York, 1987; Chapter 3, pp 63−67.
(59) Christe, K. O.; Dixon, D. A.; Sanders, J. C. P.; Schrobilgen, G. J.; Wilson, W. W. *Inorg. Chem.* **1994**, *33*, 4911.
(60) Birchall, T.; Gillespie, R. J.; Vekris, S. L. *Can. J. Chem.* **1965**, *43*, 1672.
(61) Damarius, R.; Huppmann, P.; Lentz, D.; Seppelt, K. *J. Chem. Soc., Dalton Trans.* **1984**, 2821.
(62) Jameson, C. J. In *Multinuclear NMR*; Mason, J., Ed.; Plenum Press: New York, 1987; Chapter 4, pp 102−104.
(63) Dudley, F. B.; Shoolery, J. N.; Cady, G. H. *J. Am. Chem. Soc.* **1956**, *78*, 568.
(64) (a) Berry, R. S. *J. Chem. Phys.* **1960**, *32*, 933. (b) Wasada, H.; Hirao, K. *J. Am. Chem. Soc.* **1992**, *114*, 16.

Table 2. Calculated and Predicted Geometries of POF_4^- Compared to Calculated and Observed Geometries of Isoelectronic SOF_4

	POF_4^-				SOF_4			
	SCF/DZ+P	SCF/DZ+P$^+$	LDF/DZVP2	pred	SCF/DZ+P	SCF/DZ+P$^+$	LDF/DZVP2	obsd[a]
r(X−O) (Å)	1.465	1.464	1.493	1.47	1.406	1.403	1.440	1.409
r(X−F_{eq}) (Å)	1.583	1.579	1.630	1.59	1.529	1.528	1.592	1.539
r(X−F_{ax}) (Å)	1.648	1.646	1.677	1.65	1.583	1.581	1.634	1.596
∠O−X−F_{ax} (deg)	98.3	97.93	99.4	98.6	97.2	97.36	98.2	97.7
∠F_{eq}−X−F_{eq} (deg)	113.0	112.4	114.5	113.4	111.4	111.8	111.7	112.8

[a] Values from refs 10 and 11.

state with four equivalent fluorine atoms.[65] NMR spectroscopy alone cannot distinguish between this and other mechanisms that result in the permutation of fluorine nuclei.[66,67] Other mechanisms have been favored for compounds such as ClF_3,[68] which possesses two free valence electron pairs on the central atom, or SiH_4F^- [65] and PH_4F,[69] where in the minimum energy structures, the two axial positions are occupied by one fluorine and one hydrogen ligand. Failure to slow the exchange process in POF_4^- at −140 °C and in SOF_4[47] at −150 °C indicates that both species have very low activation barriers to intramolecular exchange. This behavior contrasts with the fluxionality of PF_4^- and SF_4 for which limiting spectra have been obtained and activation barriers of 10.3 kcal mol^{-1} for PF_4^- [8] and 11.8 (neat liquid)[70] and 12.4 kcal mol^{-1} (gas phase)[71] for SF_4 have been determined by variable-temperature NMR experiments. The $\nu_4(A_1)$ and $\nu_5(A_1)$ antisymmetric combination of axial and equatorial scissoring bends in PF_4^-/SF_4 and POF_4^-/SOF_4, respectively, correspond to the motions involved in the Berry pseudorotation exchange mechanism. In PF_4^- [8] and SF_4,[72] $\nu_4(A_1)$ occurs at 210 and 228 cm^{-1}, respectively, paralleling the experimentally determined activation barriers. In POF_4^- and SOF_4,[47] the respective $\nu_5(A_1)$ modes are very similar to each other but occur at significantly lower frequencies than their tetrafluoride counterparts, i.e., 169 and 174 cm^{-1}, respectively, suggesting that the activation barriers for POF_4^- and SOF_4 are significantly lower than those in PF_4^- and SF_4. These conclusions are borne out in more detail in our theoretical calculations of the transition states and energy barriers involved in this exchange (see below).

Theoretical Calculations. Since the isolation of solid POF_4^- salts, particularly in a reasonably pure state for vibrational spectroscopy or as single crystals for X-ray diffraction, was frustrated by extreme experimental difficulties, the geometry, force fields, and some spectroscopic properties were calculated by density functional theory and molecular orbital theory at the self-consistent field (SCF) level. To test the adequacy of these calculations, the NMR shifts of POF_4^- were also calculated and compared to the observed ones. As an additional quality check and for obtaining realistic scaling factors for our methods, we have also calculated these data for the well-characterized isoelectronic SOF_4 and other closely related molecules and ions.

Geometry of POF_4^-. The geometries of POF_4^- and isoelectronic SOF_4 were calculated at the SCF/DZ+P, SCF/DZ+P$^+$, and LDF/DZVP2 levels, and the results are summarized in Table 2. Both calculations resulted in a pseudo-trigonal-bipyramidal structure of C_{2v} symmetry as the energy minimum, in accord with the experimentally known[10,11] structure of SOF_4. By analogy with our previous study[8] of the closely related PF_3 and PF_4^- species, the SCF calculations gave better results than those at the DFT level. By using the calculated and the experimentally known[10,11] SOF_4 results as a basis for correcting the calculated POF_4^- values, the following geometry, which we expect to be very close to the true geometry, is predicted for POF_4^-.

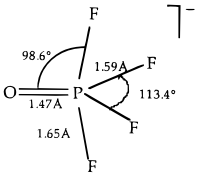

This geometry is very similar to that established[10,11] for SOF_4. The bond angles are almost identical and all bonds in POF_4^- are somewhat longer (0.05−0.07Å) than the corresponding ones in SOF_4, as expected for an increased polarity of the bonds due to the formal negative charge in POF_4^-. The compression of the F−P−F angles by the oxygen ligand, which causes a deviation from the ideal trigonal-bipyramidal geometry with 180° and 120° bond angles, is in accord with the electron domain of the P−O double bond being larger than those of the P−F single bonds.[73]

Vibrational Spectra and Force Field. The vibrational spectra of POF_4^- and SOF_4 were also calculated at the different levels of theory. As with the geometry calculations, the SCF values, after appropriate scaling, duplicated best the experimentally observed[47] spectra of SOF_4 and, therefore, were used also for POF_4^- with the scaling factors taken from SOF_4. The results are summarized in Table 3. As can be seen from this table, the spectra of POF_4^- and SOF_4 are very similar, except for the expected lowering of the frequencies in POF_4^- due to the formal negative charge which increases the polar character of the bonds in POF_4^-. The same trend was observed for the structurally closely related pair PF_4^-/SF_4 (see Table 4).

Furthermore, the calculated frequencies, IR and Ra intensities, and $^{32}S-^{34}S$ isotopic shifts (see below) require the following corrections of the assignments previously proposed[47] for SOF_4. The very weak and questionable 447-cm^{-1} IR and 455-cm^{-1} Raman bands cannot be due to $\nu_4(A_1)$, which should be of medium intensity in the IR, and probably belong to a combination band, such as $(\nu_5 + \nu_{12})(B_2) = 444$ cm^{-1}. Based on the calculated IR intensities, the medium strong 567-cm^{-1} IR band cannot be due to $\nu_9(B_1)$, which should be of almost zero IR intensity, and is reassigned to $\nu_4(A_1)$. Since $\nu_4(A_1)$, $\nu_6(A_2)$, $\nu_9(B_1)$, and $\nu_{11}(B_2)$ should all exhibit significant Raman intensities and occur within 12 cm^{-1} of each other, but only one Raman band at 566 cm^{-1} is observed in this region, a quadruple coincidence of Raman bands at 566 cm^{-1} must be assumed. The revised assignments are given in Table 3 and satisfy all

(65) Windus, T. M.; Gordon, M. S.; Burggraf, L. W.; Davis, L. P. *J. Am. Chem. Soc.* **1991**, *113*, 4356.
(66) Steigel, A. In *NMR—Basic Principles and Progress; Dynamic NMR Spectroscopy*; Diel, P., Fluck, E., Kosfeld, R., Eds.; Springer-Verlag: New York, 1978; Vol. 15, p 1 and references therein.
(67) Eisenhut, M.; Mitchell, H. L.; Traficante, D. D.; Kaufman, R. J.; Deutch, J. M.; Whitesides, G. M. *J. Am. Chem. Soc.* **1974**, *96*, 5385.
(68) Minyaev, R. M. *Chem. Phys. Lett*, **1992**, *196*, 203.
(69) Windus, T. M.; Gordon, M. S. *Theor. Chim. Acta* **1992**, *83*, 21.
(70) Gombler, W. Diploma Thesis, Saarbrücken, FRG, 1974. Gombler, W. Personal communication.
(71) Spring, C. A.; True, N. S. *J. Am. Chem. Soc.* **1983**, *105*, 7231.
(72) Sawodny, W.; Birk, K.; Fogarasi, G.; Christe, K. O. *Z. Naturforsch., B* **1980**, *35B*, 1137 and references therein.
(73) (a) Gillespie, R. J.; Robinson, A. E. *Angew. Chem., Int. Ed. Engl.* **1996**, *35*, 495. (b) Gillespie, R. J.; Bytheway, I.; DeWitte, R. S.; Bader, R. F. W. *Inorg. Chem.* **1994**, *33*, 2115.

Table 3. Calculated Vibrational Frequencies of POF_4^- Compared to Calculated and Observed Frequencies of SOF_4

IR and Raman activity	assignmt in point group C_{2v}		approx mode description	SOF_4 obsd freq, cm^{-1} (int) IR[a]	SOF_4 obsd freq, cm^{-1} (int) Raman[a]	SOF_4 calcd SCF freq (IR/Ra int) unscaled	SOF_4 calcd SCF freq (IR/Ra int) scaled[b]	POF_4^- calcd SCF freq (IR/Ra int) unscaled	POF_4^- calcd SCF freq (IR/Ra int) scaled[c]
IR, RA	A_1	ν_1	ν X=O	1380 vs	1380 (0.7)p	1471 (338/4.3)	1380	1351 (418/3.7)	1267
		ν_2	ν sym XF_{2eq}	796 m	795 (10)p	894 (59/13.8)	796	832 (62/7.3)	741
		ν_3	ν sym XF_{2ax}	588 mw	587 (1.7)p	666 (6.7/4.1)	593	540 (15/1.4)	481
		ν_4	sym comb of eq and ax δ sciss	567 ms	566 (1.7)	614 (44/1.0)	565	566 (32/0.9)	521
		ν_5	asym comb of eq and ax δ sciss		174 (0.4)	209 (0.1/0.3)	192	183 (0/0.1)	169
−, RA	A_2	ν_6	τ		566 (1.7)	600 (0/1.0)	553	535 (0/0.6)	493
IR, RA	B_1	ν_7	ν sym XF_{2ax}	819 vs	815 sh	942 (611/0.1)	839	795 (623/0)	708
		ν_8	mix of δ wag X=O and δ wag XF_{2eq}	639 ms	640 sh	691 (70/0.5)	636	619 (75/0.4)	570
		ν_9	mix of δ wag X=O and δ wag XF_{2eq}		566 (1.7)	600 (0.1/2.2)	553	526 (0.2/1.6)	484
IR, RA	B_2	ν_{10}	ν asym XF_{2eq}	926 s	924 (0.2)	1030 (319/1.3)	918	935 (368/0.3)	833
		ν_{11}	sym comb of equat rock and axial bend	558 ms	566 (1.7)	610 (44/2.3)	562	558 (51/1.7)	514
		ν_{12}	asym comb of equat rock and axial bend	270 vw	265 (0.7)	292 (0.9/1.2)	269	266 (2.7/0.7)	245

[a] Data from ref 47, except for reassigning ν_9 to ν_4, eliminating the assignment of the extremely weak and questionable 447 IR and 455 cm^{-1} Ra bands to ν_4 (A_1) and assuming a quadruple coincidence of ν_4, ν_6, ν_9, and ν_{11} at 566 cm^{-1} in the Raman spectrum. [b] The stretching and deformation frequencies were multiplied by empirical factors of 0.8908 and 0.9210, respectively, to maximize their fit with the observed frequencies, except for ν_1, which was multiplied by 0.9381 to exactly duplicate the observed frequency. [c] The empirical scaling factors from SOF_4 were applied to POF_4^-.

Table 4. Comparison of the Calculated (SCF) Vibrational Frequencies (Observed Values in Parentheses) of the Isoelectronic Pairs SOF_4/POF_4^- and SF_4/PF_4^-

XOF_4 in C_{2v}		POF_4^- [a]	SOF_4[a]	PF_4^- [b]	SF_4[b]
A_1	ν_1	1267	1380 (1380)		
	ν_2	741	796 (796)	795 (798)	(892)
	ν_3	481	593 (588)	416 (422)	(558)
	ν_4	521	565 (567)	464 (446)	(533)
	ν_5	169	192 (174)	201 (210)	(227)
A_2	ν_6	493	553 (566)	392 (−)	(−)
B_1	ν_7	708	839 (819)	523 (515)	(729)
	ν_8	570	636 (639)		
	ν_9	484	553 (566)	446 (446)	(474)
B_2	ν_{10}	833	918 (926)	746 (745)	(867)
	ν_{11}	514	562 (558)		
	ν_{12}	245	269 (270)	293 (290)	(353)

[a] Data from Table 3. [b] Data from ref 8.

the frequency, intensity, and isotopic shift requirements from our calculations.

The symmetry force constants and potential energy distribution for POF_4^- and SOF_4 are given in Tables 5 and 6, respectively. As can be seen from the potential energy distribution, ν_4 and ν_5 and also ν_{11} and ν_{12} are symmetric and antisymmetric combinations of their corresponding symmetry coordinates. Their motions can be depicted in the following way.

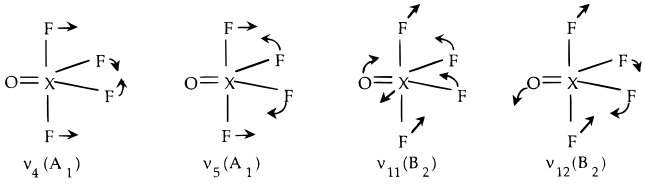

To probe the agreement of our calculated force fields with available experimental data, the ^{32}S and ^{34}S isotopic shifts were calculated from the SCF second derivatives for SOF_4. The calculated shifts were scaled by the same factors as the corresponding frequencies and are compared in Table 7 with the reported[47] experimental data. As can be seen from Table 7, our calculated isotopic shifts are in good agreement with the experimental values and support our revised assignments for SOF_4.

Since the internal stretching force constants are a measure for the bond strengths, these constants were calculated for POF_4^- and SOF_4 from the symmetry force constants of Table 5, using the explicit F matrix previously reported[47] for SOF_4. The results are listed in Table 8 and are compared to the literature values for POF_2^-,[59] PF_4^-,[8] POF_3,[74] PF_3,[75] SF_4,[72] and SOF_2.[59] In addition to the expected trends, i.e., increasing covalency and bond strength with increasing oxidation state and positive charge,[8] there is one unexpected feature. When adding an oxygen ligand to PF_4^-, the axial P−F bonds are strengthened much more than the equatorial ones. Thus, $f_r(PF_{ax})$ increases from 1.82 to 3.47 mdyn/Å and the axial bond lengths are reduced from 1.74 to 1.65 Å, while $f_r(PF_{eq})$ only increases from 3.94 to 4.96 mdyn/Å and the equatorial bond lengths are only reduced from 1.60 to 1.59 Å. A similar, although less pronounced, effect is observed for the SF_4/SOF_4 couple. It appears that the ionic character of the axial bonds, which contain strong ionic contributions and can be described as semi-ionic, three-center-four-electron bonds,[76] is reduced more by the oxidative oxygenation than that of the more covalent equatorial bonds. The increase in the equatorial bond strength from PF_4^- to POF_4^- is as expected and is comparable to that encountered on going from the predominantly covalent PF_3 to POF_3 (see Table 8).

***C_{4v}* Transition States and Energy Barriers toward Intramolecular Fluorine Ligand Exchange.** The $\nu_5(A_1)$ vibration (see above) exhibits the lowest frequency and directly leads to the C_{4v} transition state, which is the lowest energy pathway in these molecules for the equatorial−axial fluorine exchange[8] by the following Berry-type[64] pseudorotation exchange mechanism.

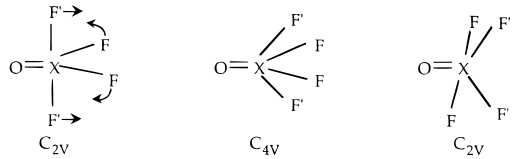

The C_{4v} transition states, which represent the activation energy barriers for this exchange,[8] were calculated for POF_4^-, SOF_4, PF_4^-, and SF_4 to support our conclusions from the above NMR data that the barriers in the XOF_4 species are significantly lower than those in the corresponding XF_4 species. The C_{4v} structures were calculated at the SCF/DZ+P level, and MP2 energies were calculated at these geometries. The vibrational frequencies were

(74) Siebert, H. *Anwendungen der Schwingungsspektroskopie in der Anorganischen Chemie, Anorganische und Allgemeine Chemie in Einzeldarstellungen VII*; Springer-Verlag: Berlin, Heidelberg, New York, 1966.
(75) Small, C. E.; Smith, J. G. *J. Mol. Spectrosc.* **1978**, *73*, 215.
(76) Pimentel, G. C. *J. Chem. Phys.* **1951**, *19*, 446. Hach, R. J.; Rundle, R. E. *J. Am. Chem. Soc.* **1951**, *73*, 4321. Rundle, R. E. *J. Am. Chem. Soc.* **1963**, *85*, 112.

Table 5. Scaled[a] SCF Force Fields[b] of POF_4^- and SOF_4

POF_4^-

	F_{11}	F_{22}	F_{33}	F_{44}	F_{55}
F_{11}	9.76				
F_{22}	0.20	5.03			
F_{33}	0.68	1.20	3.68		
F_{44}	-0.51	0.56	0.17	1.60	
F_{55}	-0.15	0.13	0.14	0.64	0.76

F_{66} = 2.08

	F_{77}	F_{88}	F_{99}
F_{77}	3.26		
F_{88}	-1.13	2.31	
F_{99}	0.67	-0.24	1.68

	$F_{10,10}$	$F_{11,11}$	$F_{12,12}$
$F_{10,10}$	4.88		
$F_{11,11}$	0.97	2.37	
$F_{12,12}$	0.18	0.50	0.64

SOF_4

	F_{11}	F_{22}	F_{33}	F_{44}	F_{55}
F_{11}	11.57				
F_{22}	0.09	5.44			
F_{33}	0.62	0.96	4.48		
F_{44}	-0.53	0.53	0.15	1.26	
F_{55}	-0.098	0.098	0.11	0.48	0.57

F_{66} = 2.44

	F_{77}	F_{88}	F_{99}
F_{77}	4.44		
F_{88}	-1.28	2.69	
F_{99}	0.79	-0.25	2.02

	$F_{10,10}$	$F_{11,11}$	$F_{12,12}$
$F_{10,10}$	5.35		
$F_{11,11}$	1.13	2.77	
$F_{12,12}$	0.16	0.53	0.68

[a] The calculated SCF force constants were scaled by multiplication with the square or product of the corresponding scaling factors given in footnote *b* of Table 3. [b] Stretching constants in mdyn/Å, deformation constants in mdyn Å/rad^2, and stretch−bend interaction constants in mdyn/rad.

Table 6. Potential Energy Distributions[a] for POF_4^- and SOF_4 Based on Their SCF Force Fields

		POF_4^-		SOF_4	
C_{2v}		freq, cm^{-1}	PED (%)	freq, cm^{-1}	PED (%)
A_1	ν_1	1267	64.3(1) + 14.5(4) + 11.5(5) + 9.4(2)	1380	55.4(1) + 20.0(4) + 15.7(5) + 8.6(2)
	ν_2	741	67.8(2) + 16.8(3) + 7.2(4) + 6.2(5) + 2.0(1)	796	62.3(2) + 15.3(3) + 10.8(4) + 9.0(5) + 2.5(1)
	ν_3	481	44.0(3) + 28.4(4) + 14.9(2) + 12.5(5)	593	65.0(3) + 14.9(2) + 11.5(4) + 7.8(5) + 0.9(1)
	ν_4	521	45.7(4)[a] + 27.1(5)[a] + 22.9(3) + 3.5(2)	565	65.1(4) + 31.1(5) + 1.9(3) + 1.9(2)
	ν_5	169	73.4(5)[a] + 26.3(4)[a]	192	75.3(4) + 24.5(5)
A_2	ν_6	493	100(6)	553	100(6)
B_1	ν_7	708	68.2(7) + 17.2(9) + 14.6(8)	839	66.8(7) + 17.3(9) + 15.8(8)
	ν_8	570	53.3(8) + 46.1(9)	636	51.7(9) + 47.6(8)
	ν_9	484	61.6(9) + 37.8(8)	553	58.1(9) + 41.7(8)
B_2	ν_{10}	833	59.2(10) + 30.4(12) + 10.4(11)	918	58.1(10) + 31.1(12) + 10.7(11)
	ν_{11}	514	63.4(12)[a] + 34.6(11)[a] + 2.1(10)	562	61.1(12) + 37.1(11) + 1.8(10)
	ν_{12}	245	80.5(12)[a] + 19.0(11)[a]	269	83.5(12) + 16.0(11)

[a] The following symmetry coordinates were used: S_1, ν X=O; S_2, ν sym XF_{2eq}; S_3, ν sym XF_{2ax}; S_4, δ sym XF_{2eq}; S_5, δ sym XF_{2ax}; S_6, τ; S_7, ν as XF_{2ax}; S_8, δ wag XF_{2eq}; S_9, δ wag X=O; S_{10}, ν as XF_{2eq}; S_{11}, δ XF_{2ax} out of OXF_{2ax} plane; S_{12}, δ rock XF_{2eq}.

Table 7. Calculated and Observed $^{32}S-^{34}S$ Isotopic Shifts of SOF_4

		freq, cm^{-1}	$\Delta\nu$ calcd, cm^{-1}	$\Delta\nu$ obsd,[a] cm^{-1}
A_1	ν_1	1380	16.3	~15[b]
	ν_2	796	2.1	
	ν_3	588	0.4	
	ν_4	567	3.1	~2.3[c]
	ν_5	174	0	
A_2	ν_6	566	0	
B_1	ν_7	819	13.6	13.1
	ν_8	639	2.9	2.4
	ν_9	566	0.1	
B_2	ν_{10}	926	13.8	14.0
	ν_{11}	558	3.2	~2.5[c]
	ν_{12}	270	0	

[a] Matrix isolation data from ref 47 with the revised assignments from Table 3. [b] The matrix IR band for $\nu_1(A_1)$ at 1376 cm^{-1} is complicated by Fermi resonance with several combination bands, adding uncertainty to the reported isotopic shift. [c] These shifts were estimated from the shoulders shown in Figure 3J of ref 47.

Table 8. Stretching Force Constants (mdyn/Å) of POF_4^- and SOF_4 Compared to Those of POF_2^-, PF_4^-, POF_3, PF_3, SF_4, and SOF_2

	POF_2^- [a]	POF_4^- [b]	PF_4^- [c]	POF_3[d]	PF_3[e]	SOF_4[b]	SF_4[f]	SOF_2[a]
f_r, eq	2.68	4.96	3.94	6.35	5.49	5.40	5.36	4.06
f_r, ax		3.47	1.82			4.46	3.25	
f(X=O)	8.34	9.76		11.38		11.57		11.12

[a] Reference 59. [b] This work. [c] Reference 8. [d] Reference 74. [e] Reference 75. [f] Reference 72.

also calculated for these transition states, and each state exhibits, as expected, one imaginary frequency ranging from 129 cm^{-1} in POF_4^- to 189 cm^{-1} in SF_4. The results are summarized in Table 9. The energies of the transition states, which represent the barriers for the equatorial−axial fluorine ligand exchange, are summarized in Table 10 and are compared to the experimental values for SF_4 and PF_4^-.[8] As can be seen from Table 10, the SCF values differ by only 1−2 kcal from the MP2 values and both agree well with the experimentally available data. Therefore, even though no experimental data are available due to the low barrier heights, the values for POF_4^- and SOF_4 are also expected to be close to the real numbers. The results from these calculations show that the barriers to axial−equatorial fluorine ligand exchange in the XOF_4 species (3.6 ± 1 kcal mol^{-1}) are indeed significantly lower than those (11.3 ± 1.1 kcal mol^{-1}) in the corresponding XF_4 species and readily account for the different exchange rates observed in the NMR experiments (see above).

The observed differences in the fluorine ligand exchange rates of POF_4^-, SOF_4, PF_4^-, and SF_4 can readily be explained from their geometries. In SOF_4 and POF_4^-, the $F_{ax}-X-F_{ax}$ and $F_{eq}-X-F_{eq}$ bond angles are already much closer to the ideal C_{4v} angle of about 142° and therefore require less deformation energy than those in SF_4 and PF_4^- to reach the C_{4v} geometry of the transition state. The sums of the angle deformations required for reaching the C_{4v} transition state geometries for these species are as follows: SF_4, 71.5°; PF_4^-, 68.4°; SOF_4, 51.8°; POF_4^-, 49.4°. This order parallels the inversion barriers that have been found (SF_4, 12 kcal/mol; PF_4^-, 10.3 kcal/mol; SOF_4, 4 kcal/mol; POF_4^-, 3 kcal mol^{-1}) and may provide a useful general relationship for the estimation of inversion barriers in similar molecules. A brief search for other low-lying transition states for POF_4^- showed that states, such as the C_{3v} geometry,

Table 9. Vibrational Frequencies, Infrared and Raman Intensities, and Geometries of the C_{4v} Transition States of POF_4^-, SOF_4, PF_4^-, and SF_4

geometry	POF_4^-	SOF_4	PF_4^-	SF_4
r(XF) (Å)	1.619	1.562	1.676	1.593
r(XO) (Å)	1.462	1.399		
∠FXF (deg)	83.7	84.1	82.0	83.2
∠OXF (deg)	109.3	108.7		

Vibrational Frequencies and Intensities

		freq, cm^{-1} (IR, RA int[a])							
	C_{4v}	unscaled	scaled[b]	unscaled	scaled[b]	unscaled	scaled[b]	unscaled	scaled[b]
A_1	ν X=O	1362 (366, 4.1)	1278	1486 (323, 4.7)	1394				
	ν sym XF_4 in phase	796 (55, 6.9)	709	860 (553, 13.7)	766	790 (183, 6.0)	704	899 (115, 13.7)	801
	δ sym XF_4	552 (50, 1.0)	508	604 (56, 1.7)	556	544 (23, 1.3)	501	615 (43, 2.4)	566
B_1	ν sym XF_4 out of phase	544 (0, 1.1)	485	649 (0, 2.9)	578	468 (0, 2.3)	417	614 (0, 4.9)	547
	δ sym XF_4 out of phase	129i	119	156i	144	173i	159	189i	174
B_2	δ sciss XF_4	582 (0, 0.7)	536	651 (0, 1.3)	600	531 (0, 0.6)	489	613 (0, 1.2)	565
E	ν sym XF_4	879 (1000, 0.2)	783	992 (940, 1.0)	884	722 (854, 5.4)	643	905 (847, 5.1)	806
	δ OXF_4	597 (111, 1.5)	550	658 (109, 1.8)	606				
	δ asym XF_4	413 (6, 2.8)	380	463 (3, 4.3)	426	493 (20, 0)	454	570 (43, 0.1)	525

[a] Ir intensities in km/mol. [b] The empirical scaling factors from Table 3, footnote *b*, were used.

Table 10. Activation Energy Barriers (kcal/mol) for the Berry-Type Exchange of Axial and Equatorial Fluorine Ligands in POF_4^-, SOF_4, PF_4^-, and SF_4

method[a,b]	species	$E(C_{2v}-C_{4v})$	$E(C_{2v}-C_{4v})$ + ZPE	exptl value
SCF	SF_4	12.4	12.3	11.8 (liquid),[c]
MP2	SF_4	10.3	10.3	12.4 (gas)[d]
SCF	PF_4^-	11.4	11.4	10.3[e]
MP2	PF_4^-	10.2	10.2	
SCF	SOF_4	5.2	5.0	
MP2	SOF_4	3.6	3.3	
SCF	POF_4^-	3.4	3.2	
MP2	POF_4^-	2.7	2.5	

[a] All calculations were carried out with the same polarized double-ζ basis set. [b] Density Functional Theory calculations were also carried out for these transition states with the same basis set and yielded values that were consistently about 2−4 kcal/mol lower than the MP2 values. [c] Reference 70. [d] Reference 71. [e] Reference 8.

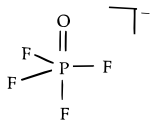

were at least 20 kcal mol^{-1} higher than the C_{4v} structure and in some cases were not transition states.

NMR Chemical Shift Calculations. NMR chemical shift calculations were carried out with the GIAO method[35] at the nonlocal BLYP level[32,33] with use of a triple-ζ basis set augmented by two polarization functions and the HF/DZVP geometries. The results for SF_4, PF_4^-, SOF_4, and POF_4^- are summarized in Table 11. Our calculated chemical shift values are consistently low by about 18 ± 7 ppm, and the chemical shift differences within a given compound are in good agreement with experiment. In view of the strong influence of conditions (such as the physical state of the compound, solvent, and temperature), the calculated values are in good agreement with the experimental ones and lend further support to our NMR spectroscopic identification of the POF_4^- anion given above. They also demonstrate that the species, having a ^{31}P shift of −10.9 ppm and previously attributed to POF_4^-,[13] cannot be due to this anion.

Chemical shift calculations were carried out also at the LORG[42] and IGLO[41] levels using a TZVP basis set (see Table 2). For POF_4^- and SF_4, the LORG ^{19}F NMR shifts show better agreement with experiment than the other two methods, but after an empirical adjustment of 18 ppm to the GIAO values, the latter method gives for all compounds the most consistent agreement with experiment.

Reaction Energies. As already pointed out above, the thermal stabilities and dismutation characteristics of isoelectronic SOF_4 and POF_4^- differ dramatically. It was important to establish whether this different behavior is due to thermodynamics or kinetics. A search of the thermochemical literature implied that the reaction energies of the POF_4^- and SOF_4 dismutation reactions differ by about 70 kcal mol^{-1}. Such a huge difference would be very remarkable for these isoelectronic systems and prompted us to examine these data in more detail.

The value of −76 kcal mol^{-1}, quoted by Larsen and McMahon for the dismutation reaction of POF_4^-,[6] was based on their fluoride ion affinity measurements. However, fluoride affinity values alone are insufficient to derive the required heats of formation of the complex anions, and one must also know the heats of formation of the neutral parent molecules. Unfortunately, these authors quoted neither the values nor the sources of the $\Delta H_f°$ values of the three necessary parent molecules, POF_3, PO_2F, and PF_5. Using the JANAF values[16,17] of −295.6 and −376.9 kcal mol^{-1} for $\Delta H_f°$ of POF_3 and PF_5, respectively, and a published value of −171.3 kcal mol^{-1} for $\Delta H_f°$ of PO_2F, which was derived from tungsten transport measurements,[14] and Larsen and McMahon's fluoride ion affinities[6] (Scheme 1), one obtains a more plausible value of −36 kcal mol^{-1} for the dismutation energy of POF_4^-, which is in excellent agreement with our values calculated by *ab initio* methods (see Table 12).

The second set of data that needed scrutiny were the heats of formation of SO_2F_2 and SOF_4 (the $\Delta H_f°$ value of SF_6 is well determined[16]). Although SO_2F_2 has been included in the JANAF tables, the selected values were based on percent conversions for reaction 9 between 110 and 700 °C, which were

$$SO_2 + Cl_2 + 2HF \rightarrow SO_2F_2 + 2HCl \qquad (9)$$

taken from a 1963 U.S. Patent.[77] However, the listed value of −181.3 kcal mol^{-1} for $\Delta H_f°$ of SO_2F_2 differs significantly from an earlier value of −205 kcal mol^{-1}, which was derived from electron impact studies[18] and was not considered for the JANAF tables based on their adoption of a poor D(S−F) value for SF_6. Similarly, the value for $\Delta H_f°$ of SOF_4 is poorly determined. There is only one experimental value of −235.7 kcal mol^{-1}, derived from tungsten transport studies,[14] and one estimated value of −228.0 kcal mol^{-1}, which is coupled to the SO_2F_2 value of −181.3 kcal mol^{-1}. The coupling of this estimate to

(77) Ruh, R. P.; Davis, R. A.; Allswede, K. A. U.S. Patent 3,092,458 (1963).

Table 11. Comparison of Calculated and Observed Chemical Shifts[a] (ppm) for SF_4, PF_4^-, SOF_4, and POF_4^-

		calculated relative chemical shift					
		GIAO/TZ2PF/BLYP		LORG/TZVP/LDFT		IGLO/TZVP/LDFT	
compd	obsd chem shift	unadjusted	adjusted[f]	unadjusted		unadjusted	
SF_4							
$^{19}F_{ax}$	97.73[b]	78.0	96	91		155	
$^{19}F_{eq}$	37.03	23.0	41	54		84	
^{33}S		493.4	511.4	478		490	
PF_4^-							
$^{19}F_{ax}$	9.3[c]	−10.1	7.9	−3.1		24	
$^{19}F_{eq}$	−46.7	−65.0	−47	−83		−57	
^{31}P	40.5	26.8	44.8	43		46	
SOF_4							
$^{19}F_{ax}$, $^{19}F_{eq}$	av 75[d]	64.3, 37.3	50.8	68.8	133, 118	126	180, 148	164
^{33}S		268.4	286.4	198		215	
^{17}O		232.4	250.4	287		283	
POF_4^-							
$^{19}F_{ax}$, $^{19}F_{eq}$	av −85.8[e]	−87.3, −102.6	−94.95	−76.95	−81, −90	−86	−47, −68	−58
^{31}P	−75.1	−101.5	−83.5	−122		−122	
^{17}O		114.9	132.9	130		128	

[a] The following standards were used for the chemical shifts: ^{19}F, $CFCl_3$; ^{31}P, PO_4^{3-}; ^{17}O, H_2O; ^{33}S, CS_2. [b] Reference 71. [c] Reference 8. [d] Reference 63. [e] This work. [f] An empirical adjustment of 18 ppm was applied to the calculated values to maximize their fit with the observed shifts.

Scheme 1

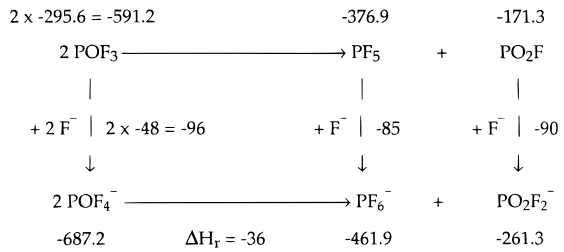

Table 12. Reaction Energies[a] (kcal mol^{-1}) for the Dismutations of POF_4^- (6), SOF_4 (7), and $ClOF_3$ (10)

	reaction energy		
computational level	POF_4^- (6)	SOF4 (7)	$ClOF_3$ (10)
BP/DZVP2	−26.4	−32.8	5.3
MP2/DZP	−31.4	−29.4	3.7
MP2/cc-VDZ	−41.5	−46.9	1.9
MP2/aug-cc-VTZ	−36.4	−45.2	1.7
CCSD(T)/cc-VDZ	−41.8	−47.1	2.5
experimental value	−36[b]		3.8[c]

[a] Electronic energy difference. HP/DZP zero-point corrections are +0.7 kcal mol^{-1} for (6), +0.8 kcal mol^{-1} for (7), and +0.5 kcal mol^{-1} for (10). [b] See text. [c] Data from ref 78.

the $\Delta H_f°$ value of −205 kcal mol^{-1} for SO_2F_2 changes the $\Delta H_f°$ estimate for SOF_4 to −216.2 kcal mol^{-1}. Depending on the choices of the $\Delta H_f°$ values for SO_2F_2 and SOF_4, the dismutation energy of SOF_4 ranges from −1.9 to −64.3 kcal mol^{-1}, with the −1.9 kcal mol^{-1} value being based on the most popular JANAF SO_2F_2[16] and the experimental SOF_4[14] values.

In view of these uncertainties in the experimental values and the general experience that reaction energies can be calculated quite accurately by *ab initio* methods due to the cancellation of systematic errors on both sides of the equations, the reaction energies were calculated for the dismutations of SOF_4 and POF_4^-. As a further test for the accuracy of our calculations, we have also computed the dismutation energy for the closely related $ClOF_3$ molecule (reaction 10).

As for SOF_4 and POF_4^-, this system involves the dismutation of two pseudotrigonal bipyramids to a pseudotetrahedron and

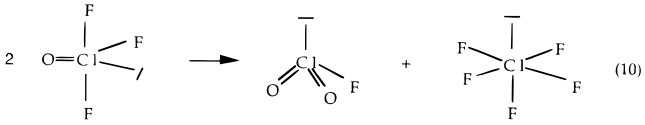

a pseudooctahedron and offers the advantage that the heats of formation of all three compounds are accurately known.[78]

The reaction energies for the dismutation reactions 6, 7, and 10 were calculated at different levels of theory, and the results are summarized in Table 12. Although the reaction energies differ somewhat with the level of theory, the following conclusions can be reached: (1) The agreement between the experimental values for $ClOF_3$ (+3.8 kcal mol^{-1}) and POF_4^- (−36 kcal mol^{-1}) with the calculated ones (+1.7 and −36.4, respectively, at the MP2/aug-cc-VTZ level) is excellent and demonstrates that the quality of the calculated values is comparable to good experimental data. (2) The dismutation reactions of POF_4^- and SOF_4 are both exothermic and of comparable energy, with SOF_4 being somewhat more exothermic than POF_4^- at each level of theory, except for MP2/DZP. Clearly, the previous literature data,[6,16] which implied a difference of about 70 kcal mol^{-1}, are badly in error, and the generally accepted values for the heats of formation of SO_2F_2[16] and SOF_4[14] and the dismutation energy of POF_4^- [6] need revision. (3) The significant difference between the reaction energies of isoelectronic SOF_4 and POF_4^- on one hand and $ClOF_3$ on the other can be rationalized by the changes in the nature of the bonding during dismutation. In pseudo-trigonal-bipyramidal SOF_4, POF_4^-, and $ClOF_3$, the two axial fluorine bonds are weak, long, semi-ionic, three-center-four-electron bonds.[76] In the SO_2F_2, $PO_2F_2^-$, SF_6, and PF_6^- dismutation products, all fluorine bonds become strong, normal, mainly covalent bonds, which causes the dismutation reaction to be highly exothermic. For $ClOF_3$, however, a free valence electron pair on chlorine is present in the ClF_5 dismutation product. This free pair seeks high s-character and induces the formation of two semi-ionic, three-center-four-electron bond pairs for the four equatorial fluorine ligands.[79] Therefore, for the $ClOF_3$ dismutation, the number of semi-ionic, three-center-four-electron bonds remains unchanged, and hence the reaction is essentially thermally neutral. The difference between molecules containing semi-ionic, three-center-four-electron bonds and others that contain either a different number or none can give rise to bad estimates for the

(78) Barberi, P. *B. I. S. T. Commissariat a l'Energie Atomique (France)* **1976**, *7*, 511.
(79) Christe, K. O. *XXIVth Int. Congr. Pure Appl. Chem.* **1974**, *IV*, 115.

thermodynamic properties, if only the total number and not the types of fluorine bonds are considered.

The influence of the computational levels on the reaction energies is relatively minor due to the cancellation of errors on both sides of the equation. Nevertheless, the following trends were observed. The MP2/cc-VDZ calculations result in more negative values than those at the MP2/DZVP level. The difference between the CCSD(T) and MP2 results with the cc-VDZ basis set is small. Improvement of the basis set leads to a decrease in the overall exothermicity, with the larger decrease found for (6), the POF_4^- reaction. The results with the larger basis sets also show that the SOF_4 dismutation is somewhat more exothermic than that of POF_4^-.

Mechanism of the Dismutation Reaction of POF_4^-. In the previous section it was demonstrated that the dismutation reactions of SOF_4 and POF_4^- are both highly exothermic and of similar magnitude. Consequently, the great difference in their dismutation behavior cannot be due to thermodynamics but must be ascribed to kinetic effects. In this section, therefore, the likely reaction mechanisms of these reactions will be scrutinized.

The low-temperature NMR studies (see above) provide an insight into the mechanism of the POF_4^- dismutation. With increasing temperature, the intensities of the POF_4^- and POF_3 signals decrease, while those due to the $[OF_2POPF_5]^-$ anion increase, indicating that POF_4^- reacts with POF_3 to yield $[OF_2POPF_5]^-$. The most likely path for this reaction is shown in (11) and involves the formation of an intermediate oxygen

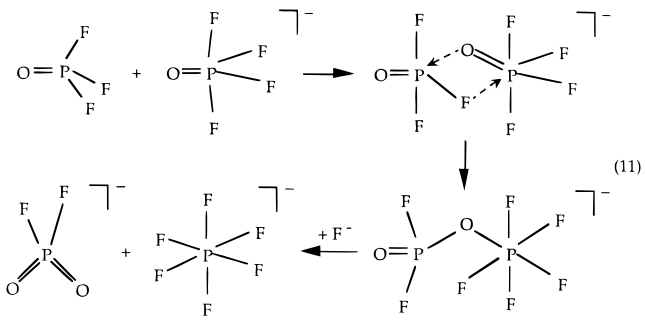

(11)

and fluorine bridged dimeric anion, which can rearrange to $[OF_2POPF_5]^-$ by allowing the bridging oxygen to form two single bonds and breaking one original P−F bond of POF_3. On further warm up, the resulting $[OF_2POPF_5]^-$ anion can readily lose its PF_5 molecule to the more basic F^- ion present as $N(CH_3)_4^+F^-$ in these solutions, resulting in the formation of the final species, $PO_2F_2^-$ and PF_6^-.

This mechanism involves exclusively low activation energy steps (F^- ion transfer and donor−acceptor interactions) and thus explains the great ease of the POF_4^- dismutation even at the very low temperatures. Since the dismutation requires the presence of free POF_3 for the formation of the crucial dimeric $[OF_2POPF_5]^-$ anion, it is predicted that in the absence of free POF_3, a well-isolated POF_4^- anion will be a stable species that can be isolated at ambient temperature. Synthetic approaches would involve the uses of excess F^- and of low temperatures where all POF_3 can be converted to POF_4^- before the dismutation sets in.

The second question to be addressed is why POF_4^- dismutates so readily and isoelectronic SOF_4 does not. Application of mechanism 11 to the isoelectronic sulfur species would require an SOF_3^+ cation and an SOF_4 molecule for the generation of an intermediate $[OF_2SOSF_5]^+$ dimeric cation that could either eliminate SO_2F_2 with formation of an energetically highly unfavorable SF_5^+ cation or undergo attack by an F^- anion to give SF_6 and SO_2F_2 (reaction 12).

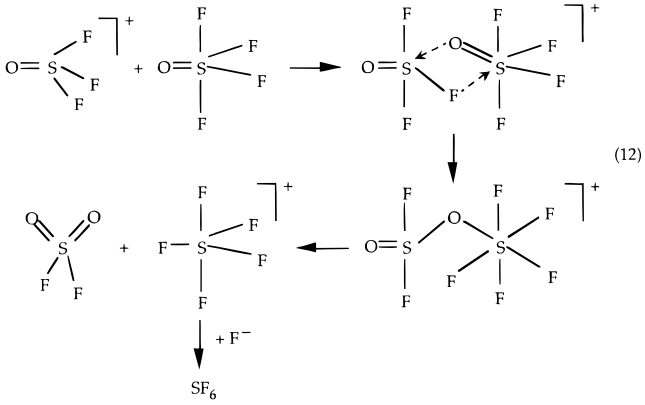

(12)

Contrary to the POF_3 dismutation which is F^- catalyzed, the SOF_4 dismutation would require very strong Lewis acids such as SbF_5 or AsF_5 as catalysts. Clearly, mechanism 12 would involve several energetically very unfavorable species, such as SF_5^+ or polycations containing SOF_4, and, therefore, should exhibit high activation energy barriers.

Starting the dismutation of SOF_4 with two SOF_4 molecules is equally unattractive. The substitution of one doubly bonded oxygen ligand by two singly bonded fluorine ligands would require a dimeric intermediate with one oxygen and two fluorine bridges and one heptacoordinated sulfur atom (reaction 13).

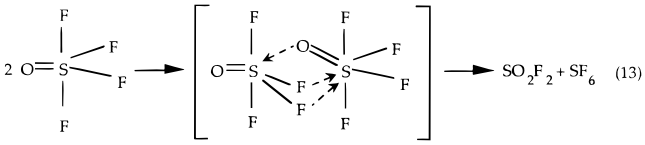

(13)

Therefore, the SOF_4 dismutation to SO_2F_2 and SF_6 is mechanistically unfavorable and is not observed under normal conditions.

Conclusion

The ephemeral POF_4^- anion has been prepared and identified for the first time. Whereas its geometry and spectroscopic properties mimic the isoelectronic SOF_4 molecule, its chemical behavior and, in particular, its dismutation to XO_2F_2 and XF_6 type species are very different. The POF_4^- anion is thermally highly unstable and starts to dismutate even at −140 to −130 °C to $PO_2F_2^-$ and PF_6^-, whereas SOF_4 is kinetically stable toward dismutation to SO_2F_2 and SF_6. Extensive use of theoretical calculations was made to better understand the properties and reactions of the highly unstable POF_4^- anion. Of particular interest in this respect were its fluxionality, i.e., the equatorial−axial fluorine exchange, and its dismutation process.

Acknowledgment. This paper is dedicated to the memory of Dr. Charles B. Lindahl, a former Rocketdyne colleague, coworker, and friend. The authors thank Prof. G. A. Olah and Dr. S. L. Rodgers for their active support. The work at the Phillips Laboratory was financially supported by the Propulsion Directorate of the U. S. Air Force, that at USC by the National Science Foundation, that at McMaster University by the Natural Sciences and Engineering Research Council of Canada, and that at Pacific Northwest National Laboratory under the auspices of the Office of Basic Energy Sciences, U.S. Department of Energy under Contract DE-AC06-76RL01830 with Battelle Memorial Institute, which operates the Pacific Northwest Laboratory, a multiprogram national laboratory operated for the U.S. Department of Energy.

JA963421I